ISSN 0915-633X

NATIONAL INSTITUTE FOR FUSION SCIENCE

Ideal and Conventional Feedback Systems for RWM Suppression

V.D. Pustovitov

(Received - Dec. 27, 2001)

NIFS-723 Jan. 2002

RESEARCH REPORT
NIFS Series

TOKI, JAPAN

Ideal and Conventional Feedback Systems for RWM Suppression

V.D. Pustovitov

National Institute for Fusion Science, Oroshi-cho, Toki-shi, Gifu-ken 509-5292 Japan

Permanent address: Institute of Nuclear Fusion, Russian Research Centre "Kurchatov Institute", Kurchatov sq., 1, Moscow, 123182, Russian Federation

Abstract

Feedback suppression of resistive wall modes (RWM) is studied analytically using a model based on a standard cylindrical approximation. Two feedback systems are compared: 'ideal', creating only the field necessary for RWM suppression, and 'conventional', like that used in the DIII-D tokamak and considered as a candidate for ITER. The widespread opinion that the feedback with poloidal sensors is better than that with radial sensors is discussed. It is shown that the 'conventional' feedback with radial sensors can be effective only in a limited range, while using the input signal from internal poloidal sensors allows easy fulfilment of the stability criterion. This is a property of the 'conventional' feedback, but the 'ideal' feedback would stabilise RWM in both cases.

Keywords: resistive wall modes (RWM), cylindrical approximation, feedback suppression

1. Introduction

Resistive wall modes (RWM) can limit achievable beta below acceptable level in advanced tokamaks with low internal inductances [1-7]. Theory predicted that the danger could be avoided by using a feedback control of RWM. Simulations show, for example, that such a control can significantly raise the $n = 1$ ideal MHD beta limit, up to $\beta_N = 5$ or twice the no-wall limit [7]. Though theory was always optimistic, it took several years of studies in DIII-D [1-3,5] before it was reported [8] that, in experiments with active control, it became possible to sustain a discharge at pressures approaching twice the no-wall limit.

Dramatic improvements in active control in experiments in 2001 have been explained [8] as resulting owing largely to an extensive new set of magnetic sensors installed inside the vacuum vessel after the 2000 campaign.

The importance of proper positioning and orientation of magnetic sensors in the problem of the feedback control of RWM was earlier discovered numerically [6-9]. The conclusion, first stated in [6] and confirmed in subsequent studies [7-9], was that the feedback system with sensors measuring the poloidal field is much better than that with the radial-field sensors. With solid proofs, including experimental confirmation [8], the conclusion cannot raise any doubt. But some basic questions remain unanswered. For example, it follows from $\mathrm{div}\,\mathbf{B} = 0$ that poloidal and radial components of the plasma-produced helical magnetic perturbation must be (approximately) equal. Why then 'sensors measuring the poloidal field perturbations are superior to radial sensors' [7]? Is it a general rule or a property of the considered feedback schemes? These questions must be answered in the course of designing the RWM feedback system for high-beta long-pulse toroidal systems, in particular, for ITER or ITER-like large tokamaks.

One reason of superiority of the internal poloidal over radial sensors has been explained recently [10]: The poloidal component of the perturbation inside the vessel is always larger than the radial one. Larger signal can be detected easier, and feedback stabilisation can start earlier. This is certainly an advantage, but cannot be the only reason of the mentioned 'Dramatic improvements in active control capability' in recent experiments in DIII-D [8]. This can be said because the analysis [10] did not reveal any serious disadvantage of the feedback system with radial sensors. Precisely, the analysis demonstrated that both feedback systems, with radial or internal poloidal sensors, must be equally good in suppressing RWM, just different gains would be needed.

The analysis [10] has been performed using a standard cylindrical approximation [11-13], and magnetic perturbation has been described by a single harmonic. Such a case can be called 'ideal'. In the ideal case, the feedback system must produce the helical harmonic identical to the unstable mode, and nothing more. This would require stellarator-like helical windings, but for practical applications much more simple geometry is always considered: coils consisting of frame-like rectangular segments [3-9,14-19], as shown in Figure 1 [4]. Such a choice is justified, at least, by the fact that finally it provides the desired RWM suppression in theory and in DIII-D experiments. However, such simple correction coils are not optimal. As shown in [6], a single poloidal array of active coils is rather effective at stabilising the RWM, but the spectrum of the feedback-produced field is different from that of the original RWM, see Figure 2 (Fig. 10 in [6]). The difference appears because RWM has a helical structure while the rectangular active coils are aligned toroidally. Figure 3 (Figures 1 and 2 in [16]) explicitly demonstrates a difference between toroidally oriented currents in active 'window-pane' coils and helical structure of the surface current induced in the wall during RWM growth in the DIII-D tokamak. Non-optimal active coils generate side-band harmonics, different from the intrinsically unstable principle harmonic, which was ranked as the principal failure mechanism fraught with danger that the feedback might fail [17]. This failure can be illustrated by one of the simulation results for current-driven RWM in cylindrical configuration with Wesson safety factor profile [19].

Here we compare stabilising properties of the ideal and conventional feedback systems. For certainty, we call conventional a feedback system with correction coils similar to those used in DIII-D [5,8,16], with up-down symmetry with respect to the equatorial plane, evenly spaced, and with equal opposite currents in symmetrical toroidally oriented conductors, as shown schematically in Figure 1. It is known that even in the case of DIII-D (six active coils each covering a 60-degree toroidal arc) the feedback field can be modelled approximately by a single harmonic in toroidal angle ζ [16]. Therefore, the toroidal discreteness can be disregarded in the analysis.

2. General properties of a conventional feedback

The definition 'conventional' reflects the fact that such a system is used in DIII-D and considered as a candidate for ITER. The definition can be applied also to the feedback with thirty control coils providing larger poloidal but incomplete toroidal coverage in HBT-EP tokamak [15] and to almost all feedback systems considered theoretically. These include modifications of the existing DIII-D system with different coverage and the number of coil segments [9,16,18], a system consisting of a large number of evenly spaced rectangular saddle coils with toroidally symmetric distribution [14,17], a system schematically shown in Figure 1 with number of saddle coils sufficient for modelling the feedback current as a single $n=1$ harmonic [4,6,7,16].

In the latter case, generally similar to DIII-D feedback system, the feedback coils are modelled as a pair of wires carrying the oppositely directed toroidally modulated currents J_f [20]:

$$j_z^f = J_f \delta(r-r_f)\frac{\delta(\theta-\theta_c)-\delta(\theta+\theta_c)}{r_f}\exp(in\zeta). \tag{1}$$

Here θ and ζ are the poloidal and toroidal angles, respectively, so that r, θ and $z=R\zeta$ are the usual cylindrical coordinates ($2\pi R$ is the total length of the system).

A conventional feedback system can be described by several symmetric pairs of coils similar to (1) with a general property

$$j_z^f(\theta) = -j_z^f(-\theta). \tag{2}$$

In this case,

$$\psi^f(\theta) = -\psi^f(-\theta), \tag{3}$$

where ψ^f is the flux function related to the magnetic field $\mathbf{b}^f$ produced by the active coils by

$$\mathbf{b}^f = \nabla\psi^f \times \mathbf{e}_z, \tag{4}$$

$\mathbf{e}_z$ is the unit vector in z direction.

It follows from (3), (4) that

$$b_r^f(\theta) = b_r^f(-\theta), \tag{5}$$

$$b_\theta^f(\theta) = -b_\theta^f(-\theta). \tag{6}$$

These general properties of a conventional feedback system describe a symmetry of $\mathbf{b}^f$ different from the helical symmetry of the unstable RWM.

3. Theoretical model

We use a model described in detail in Ref. [13]. The model is based on a standard cylindrical approximation [11,12]. In [12,13], a single harmonic of perturbation of the magnetic field has been considered. Here we assume that the radial component b_r of the perturbed magnetic field is a combination of several harmonics:

$$b_r = \sum b_k(r)\exp[i(k\theta - n\zeta) + \gamma t]. \tag{7}$$

Here γ is the growth rate, t is the time, r, θ and $z = R\zeta$ are the same cylindrical coordinates as defined in (1).

In vacuum gaps outside the plasma, the perturbation b_r can be described as consisting of two parts, due to inner and outer sources. Accordingly,

$$b_k = b_k^{in} + b_k^{out}. \tag{8}$$

The contributions from inner and outer regions to b_r have different radial behaviour,

$$b_k^{in} = B_k^{in} x^{-\kappa-1}, \tag{9}$$

$$b_k^{out} = B_k^{out} x^{\kappa-1}, \tag{10}$$

where

$$x = r/r_w, \qquad \kappa = |k|,$$

B_k^{in} and B_k^{out} are the values of b_k^{in} and b_k^{out}, respectively, at $r = r_w$, and r_w is the radius of the resistive wall. If there are several resistive walls, r_w is the radius of the wall facing the gap where Eqs. (9) and (10) are applied. Two-wall case with ideal feedback system has been studied in [13]. Here a configuration with a single resistive wall is analysed.

At the resistive wall, considered as a thin shell $r = r_w$, two conditions must be satisfied:

$$[\![b_k]\!] = 0, \qquad [\![rb_k']\!] = \hat{\gamma} B_k. \tag{11}$$

Here $[\![X]\!] \equiv X\big|_{r-0}^{r_w+0}$ is a jump in the function across the wall, the prime is the radial derivative, $\hat{\gamma} = \gamma\tau_w$, $\tau_w = \mu_0\sigma_w d_w r_w$ is the time constant of the wall, σ_w and d_w are, respectively, its conductivity and thickness, $B_k = b_k(r_w)$ is the amplitude of the k th harmonic of the perturbation at the wall created by all sources:

$$B_k = B_k^{in} + B_k^{out}. \tag{12}$$

For more details see, for example, [13].

It follows from (9), (10) that on the outer side of the wall

$$rb_k'\big|_{r_w+0} = -(\kappa+1)B_k + 2\kappa B_k^{ext}, \tag{13}$$

where $B_k^{ext} = b_k^{out}\big|_{r_w+0}$ is the part of B_k due to the field produced by all sources outside the wall. If there is only one resistive wall, this external field is the field produced by the feedback system.

With (13), Eqs. (11) lead to

$$(\hat{\gamma} - \Gamma_k)B_k = 2\kappa B_k^{ext}. \tag{14}$$

Here the value

$$\Gamma_k \equiv -\frac{rb_k'}{b_k}\bigg|_{r_w-0} - (\kappa+1) \tag{15}$$

must be calculated on the inner side of the wall.

The system of equations (14), describing the perturbed magnetic field at the position of the resistive wall, can be a starting point for the stability analysis if the parameters Γ_k are determined for all harmonics and the feedback-produced field is given.

4. The measured signals

For analysis of the RWM feedback stabilisation, Eqs. (14) must be supplemented by the feedback algorithm. The latter must describe the feedback-produced magnetic field as a function of some input signal. RWM instability reveals itself in a magnetic perturbation outside the plasma, and the input signal can be combined of the magnetic signals measured outside the plasma.

For certainty, assume that the measurements are performed by the local probes located on the mid-plane, $\theta = 0$. The radial probes in this plane can measure the total radial field

$$b_r(r,0) = \sum_{k>0}(b_k + b_{-k})\cos n\zeta. \tag{16}$$

We use Eq. (7) with real b_k and suppress the factor $\exp(\gamma t)$ here.

Using expressions (7)-(10) for b_r, from $\mathrm{div}\,\mathbf{B} = 0$ we obtain for the poloidal component of the perturbation

$$b_\theta = -\frac{\partial}{\partial r}\int rb_r d\theta = i\sum\frac{\kappa}{k}\left(b_k^{out} - b_k^{in}\right)\exp[i(k\theta - n\zeta) + \gamma t]. \tag{17}$$

The poloidal probes in the mid-plane ($\theta = 0$) can measure

$$b_\theta(r,0)=\sum_{k>0}\left[b_k^{out}-b_k^{in}-\left(b_{-k}^{out}-b_{-k}^{in}\right)\right]\sin n\zeta\,. \tag{18}$$

In DIII-D the probes are located at the wall [5,8,9], $r=r_w$. The same wall position was assumed in [4,6,7], see. Figure 1. Following this, in addition to $\theta=0$ we put $r=r_w$ in (16) and (18). In this case, when two harmonics only, (m,n) and $(-m,n)$, are present, the measurements allow to find

$$I_r=B_m+B_{-m}, \tag{19}$$

$$I_\theta=B_m^{in}-B_m^{out}-\left(B_{-m}^{in}-B_{-m}^{out}\right)=B_m-B_{-m}-2\left(B_m^{out}-B_{-m}^{out}\right). \tag{20}$$

The first value can be measured by the radial probes, and the second can be found using poloidal probes measuring $-b_\theta(r,0)$. Minus is introduced here in order to make signs of I_r and I_θ the same. These values can be used as the input signals for the feedback control.

The radial field is continuous, and I_r is the same on both sides of the thin wall. But b_θ may be different on the different sides of the wall with a jump produced by the current induced in the wall:

$$\mu_0\mathbf{K}=\mathbf{n}\times(\mathbf{B}^{out}-\mathbf{B}^{in})\,. \tag{21}$$

Accordingly, the values I_θ^{in} and I_θ^{out} measured by the poloidal probes inside and outside the vessel, respectively, are different when $\mathbf{K}\neq 0$:

$$I_\theta^{out}=B_m-B_{-m}-2\left(B_m^f-B_{-m}^f\right), \tag{22}$$

$$I_\theta^{in}=I_\theta^{out}-2\left(B_m^w-B_{-m}^w\right). \tag{23}$$

Here $B_{\pm m}^w$ are the amplitudes of $\pm m$ harmonics of radial field produced by the currents induced in the wall. These values can be easily expressed through the harmonics of the total field using Eqs. (9)-(11):

$$B_{\pm m}^w=-\frac{\hat\gamma}{2\mu}B_{\pm m}\,. \tag{24}$$

Without feedback ($B_m^f=B_{-m}^f=0$) $\hat\gamma=\Gamma_m$, $B_{-m}=0$, and

$$\frac{I_\theta^{out}}{I_r}=1\,,\qquad \frac{I_\theta^{in}}{I_r}=\frac{\Gamma_m+\mu}{\mu}\,. \tag{25}$$

The latter expression shows that Γ_m can be determined experimentally by measuring the perturbation amplitudes. Another way is the direct measurement of the growth rate.

Since I_θ^{in} is the largest of three measured signals, internal poloidal probes are the best

choice from the viewpoint of sensitivity of the feedback system [10]. Larger input signal also results in smaller gains of the controller. Theoretical analysis [10] did not reveal any other advantage of using the signal from the internal poloidal probe: it was shown that the RWM stabilisation is equally possible with radial or external poloidal probes. But this conclusion obviously conflicts with the mentioned numerical [6-9] and experimental [8,9] results showing not only natural quantitative, but an essential difference between systems with radial and internal poloidal probes. The contradiction can be attributed to the fact that the analysis [10] was performed for the ideal feedback, while the conventional feedback used in experiments and in computations has other properties. We compare the efficiency of the RWM suppression by ideal or conventional feedback using I_r and I_θ^{in} as input signals.

5. One resistive wall, ideal feedback

This case is described in detail in [10,13]. Here we briefly summarise the main results necessary for our analysis.

If only one resistive wall is present, the external field in Eq. (14) is the field produced by the feedback system, $B_k^{ext} = B_k^f$. For a single unstable mode $k = m$ Eq. (14) gives

$$\hat{\gamma} = \Gamma_m + 2\mu B_m^f / B_m , \tag{26}$$

where $\mu = |m|$, $\Gamma_m > 0$ is the no-feedback growth rate, and B_m is the amplitude of the mode.

RWM is suppressed when $\hat{\gamma} < 0$. Assuming a simple proportional control

$$B_m^f = -K \times I , \tag{27}$$

we can compare the feedback stabilisation with input signals I from the radial probes in the mid-plane (I_r), and from poloidal probes measuring $-b_\theta(r,0)$ inside and outside the vessel (I_θ^{in} and I_θ^{out}) [10].

An ideal feedback system would create only necessary (m,n) harmonic. In this case

$$I_r = B_m , \qquad I_\theta^{in} = (1+\Gamma_m/\mu)B_m , \qquad I_\theta^{out} = I_\theta^{in} - \hat{\gamma}B_m/\mu . \tag{28}$$

The values I_θ^{in} and I_θ^{out} are expressed through B_m using Eqs. (8)-(11) and $\mathrm{div}\,\mathbf{B} = 0$ [10].

It follows from (26) that any choice from (28) would allow RWM suppression with algorithm (27). For I_r taken as input signal the stability criterion is

$$K > K_0 \equiv \Gamma_m/(2\mu) . \tag{29}$$

Since I_θ^m differs from I_r by a constant multiplier only, smaller gain K is needed when internal poloidal sensors are used:

$$K > K_0 \frac{\mu}{\mu + \Gamma_m}. \tag{30}$$

In other respects the feedback systems with radial or internal poloidal sensors are equivalent.

This is true for the ideal case. But relations (28) may not be valid for a real feedback.

6. One resistive wall, conventional feedback, radial sensors

In the ideal case, the feedback system must produce only the same helical harmonic as the plasma-generated perturbation. This would require stellarator-like helical windings. In practice, the correction coils consisting of frame-like rectangular segments [3-9,14-19] are always considered for tokamaks, see Figure 1. Such coils, called here conventional, allow the desired RWM suppression in theory and in DIII-D experiments, but they are not optimal: RWM has a helical structure while the rectangular active coils are aligned toroidally. Non-optimal active coils generate side-band harmonics, different from the intrinsically unstable principal harmonic. This harmonics can contribute to the measured input signals I, affecting the dispersion relation (26) through (27) or another feedback algorithm.

A real feedback system in addition to necessary (m,n) harmonic generates a number of side-band harmonics. Conventional feedback has a property (5) meaning that the spectrum of b_r^f is symmetric, $b_k^f = b_{-k}^f$. Therefore, even if a system is somehow optimised for stabilising (m,n) mode, at least $(-m,n)$ side-band harmonic in b_r^f must be taken into account. With two harmonics of the field from active coils, Eq. (26) must be considered together with

$$\hat{\gamma} = \Gamma_{-m} + 2\mu B_{-m}^f / B_{-m}. \tag{31}$$

Instability of a single mode means that without feedback $\Gamma_m > 0$, but $\Gamma_{-m} < 0$.

Actually, Eq. (26) alone could be used for analysis of the feedback suppression of RWM if B_m^f / B_m would be given as a function of $\hat{\gamma}$. That might be possible if B_m could be measured, which is the case of single-mode instability and an ideal feedback producing the same (m,n) harmonic. In a general case, a prescribed feedback algorithm can give B_m^f as a function of some measured signal, input for the feedback. So, Eq. (31) is needed because the side-band $(-m,n)$ harmonic affects the measurements closing the feedback chain.

If the feedback field is described by two harmonics, (m,n) and $(-m,n)$, and $B^f_{-m} = B^f_m$,

$$I_r = B_m + B_{-m} = 2B_m \frac{\hat{\gamma} - \hat{\gamma}_{cr}}{\hat{\gamma} - \Gamma_{-m}}, \tag{32}$$

where

$$\hat{\gamma}_{cr} = 0.5(\Gamma_{-m} + \Gamma_m). \tag{33}$$

With (32) and (27), Eq. (26) turns into quadratic equation for $\hat{\gamma}$:

$$\hat{\gamma}^2 + 2\hat{\gamma}(2\mu K - \hat{\gamma}_{cr}) + \Gamma_m\Gamma_{-m} - 4\mu K\hat{\gamma}_{cr} = 0. \tag{34}$$

For RWM stability, both roots of (34) must be negative. This requires two conditions,

$$\hat{\gamma}_{cr} < 0 \tag{35}$$

and

$$K > K_0(1 - 0.5\Gamma_m/\hat{\gamma}_{cr}). \tag{36}$$

The necessary gain K becomes infinitely large when $\hat{\gamma}_{cr} \to 0$ because the measured input signal I_r vanishes at $\hat{\gamma} = \hat{\gamma}_{cr}$. When $\hat{\gamma}_{cr}$ becomes positive, the unstable (m,n) mode cannot be stabilised by the conventional feedback described by (27) with $I = I_r$.

7. One resistive wall, conventional feedback, internal poloidal sensors

If the feedback field is described by two harmonics with $B^f_{-m} = B^f_m$,

$$I^{in}_\theta = B_m\left(1 + \frac{\hat{\gamma}}{\mu}\right)\frac{\Gamma_m - \Gamma_{-m}}{\hat{\gamma} - \Gamma_{-m}}. \tag{37}$$

With this input signal and proportional control (27), Eq. (26) turns into

$$(\hat{\gamma} - \Gamma_m)(\hat{\gamma} - \Gamma_{-m}) = -2K(\hat{\gamma} + \mu)(\Gamma_m - \Gamma_{-m}). \tag{38}$$

The growth rate $\hat{\gamma}$ becomes negative when $K > \max\{K_1, K_2\}$, where

$$K_1 = \frac{K_0}{1 - \Gamma_m/\Gamma_{-m}}, \qquad K_2 = \frac{\hat{\gamma}_{cr}}{\Gamma_m - \Gamma_{-m}}, \tag{39}$$

K_0 is given by (29) and $\hat{\gamma}_{cr}$ by (33).

This scheme is much better than the feedback with radial sensors since it allows suppression of RWM without restrictions on plasma parameters, and smaller gain is required.

8. Summary

The analysis gives a natural explanation of the observation that, for the RWM feedback control, 'sensors measuring the poloidal field perturbations are superior to radial sensors' [7].

The poloidal component of the perturbation inside the vessel is always larger than the radial one, see (25). Therefore, internal poloidal sensors are better for the RWM feedback control since a measured (input) signal must be above some detection level. From this viewpoint, the best input signal would be a combination $I_\theta^{in} + I_r$.

An ideal feedback system could be effective in suppressing RWM with either I_r or I_θ^{in}, just different gains K would be needed. But realistic feedback system generates side-band harmonics that influence the measurements. As a result, the conventional feedback system with radial sensors cannot suppress RWM when $\hat{\gamma}_{cr} > 0$. This value, defined by (33), is determined by plasma parameters and can vary during the discharge evolution. It can lead to increase in the necessary gain (36) above the permissible level. That may be a reason of the loss of the control observed in DIII-D experiments with radial sensors [5]. The weak point of such a feedback is aggravated when a second resistive wall is present [13]. The second wall, located between the first wall and active coils like that in ITER [21], increases the total resistive decay time decreasing thereby the RWM growth rate. Also, the second wall acts as a screen affecting penetration of the field from the active coils to the first wall. This can weaken the stabilizing influence of the feedback system even in the ideal case.

However, with internal poloidal probes the conventional feedback allows suppression of RWM without fail and at rather modest gains, see (39). The difference between two cases, related to properties (5) and (6), may be a reason of the dramatic improvements in active control in DIII-D experiments in 2001 [8].

References

[1] Strait E. J., et al., Nucl. Fusion **39** (1999) 1977.

[2] Garofalo A.M., et al., Phys. Rev. Lett. **82** (1999) 3811.

[3] Garofalo A.M., et al., Phys. Plasmas **6** (1999) 1893.

[4] Liu, Y. Q., Bondeson, A., Phys. Rev. Lett. **84** (2000) 907.

[5] Garofalo A., et al., Nucl. Fusion **40** (2000) 1491.

[6] Liu Y.Q., Bondeson A., Fransson C.M., Lennartson B., Breitholtz C., Phys. Plasmas **7** (2000) 3681.

[7] Bondeson A., Liu Y.Q., Fransson C.M., Lennartson B., Breitholtz C., Taylor T.S., Nuclear Fusion **41** (2001) 455.

[8] Johnson L.C., et al., Proc. 28th EPS Conference on Controlled Fusion and Plasma Physics, Madeira, Portugal, June 18-22, 2001. http://www.cfn.ist.utl.pt/EPS2001/fin/pdf/P4.008.pdf

[9] Okabayashi M., et al., Phys. Plasmas **8** (2001) 2071.

[10] Pustovitov V.D., "Comparison of RWM feedback systems with different input signals", Report of ITER Physics Design Group at RRC "Kurchatov Institute", Task 3, July 2001.

[11] Wesson J.A., Nucl. Fusion **18** (1978) 87.

[12] Okabayashi M., Pomphrey N., Hatcher R.E., Nucl. Fusion **38** (1998) 1607.

[13] Pustovitov V.D., Plasma Phys. Rep. **27** (2001) 195.

[14] Fitzpatrick R., Yu E. P., Phys. Plasmas **5** (1998) 2340.

[15] Cates C., et al., Phys. Plasmas **7** (2000) 3133.

[16] Chance M.S., Chu M.S., Okabayashi M., in Fusion Energy 2000 (Proc. 18th Int. Conf. Sorrento, 2000), CD-ROM, IAEA, Vienna (2001) IAEA-CN-77/THP2/01, http://www.iaea.org/programmes/ripc/physics/

[17] Fitzpatrick R., Phys. Plasmas **8** (2001) 871.

[18] Bialek J., Boozer A.H., Mauel M.E., and Navratil G.A., Phys. Plasmas **8** (2001) 2170.

[19] Hogun Jhang, Ku S.H., and Jin-Yong Kim, Phys. Plasmas **8** (2001) 3107.

[20] Bondeson A., Liu Y.Q., Gregorato D., Gribov Y., Pustovitov V.D., "Active Control of Resistive Wall Modes in the Large Aspect Ratio Tokamak", submitted to Nuclear Fusion, 2001.

[21] ITER Physics Basis, Nucl. Fusion **39** (1999) 2137.

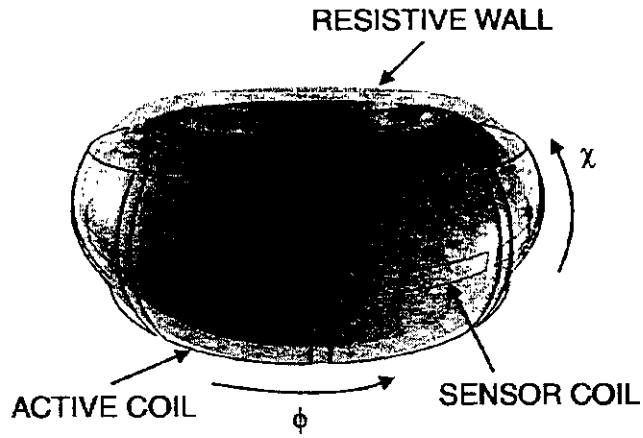

Figure 1, from [4]. Geometry of a tokamak with a ***conventional*** feedback system for nonaxisymmetric modes.

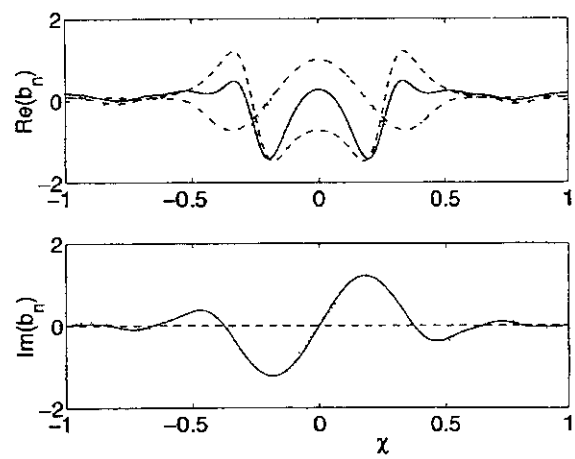

Figure 2, from [6]. The normal component of the perturbed magnetic field in two toroidal planes as a function of the normalised poloidal angle, calculated for JET equilibrium. The dotted line represents the original field without feedback; solid line, total field with feedback; dashed line, field due to the feedback coil; dashed-dotted line, plasma response field

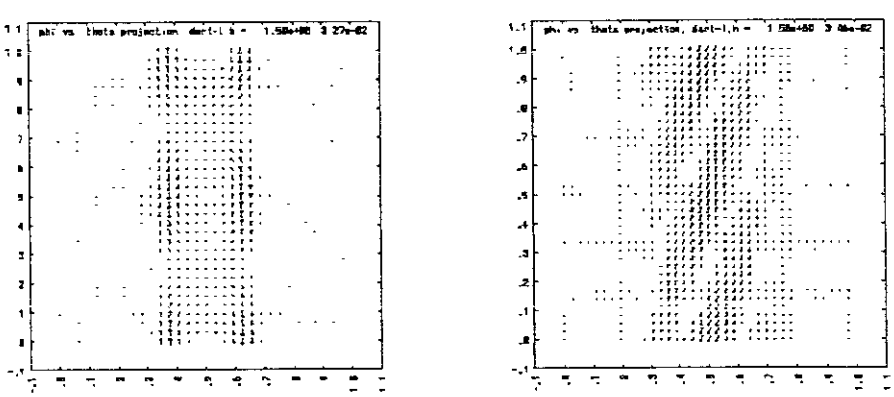

Figure 3, from [16]. The feedback coil current (left) and the induced current on the resistive shell (right) in DIII-D tokamak.

Recent Issues of NIFS Series

NIFS-702 K Ohkubo
Hybrid Modes in a Square Corrugated Waveguide
June 2001

NIFS-703 S -I Itoh and K Itoh
Statistical Theory and Transition in Multiple-scale-lengths Turbulence in Plasmas
June 2001

NIFS-704 S Toda and K. Itoh
Theoretical Study of Structure of Electric Field in Helical Toroidal Plasmas
June 2001

NIFS-705 K Itoh and S-I. Itoh
Geometry Changes Transient Transport in Plasmas
June 2001

NIFS-706 M. Tanaka and A Yu. Grosberg
Electrophoresis of Charge Inverted Macroion Complex Molecular Dynamics Study
July 2001

NIFS-707 T-H Watanabe, H Sugama and T Sato
A Nondissipative Simulation Method for the Drift Kinetic Equation
July 2001

NIFS-708 N. Ishihara and S Kida
Dynamo Mechanism in a Rotating Spherical Shell. Competition between Magnetic Field and Convection Vortices
July 2001

NIFS-709 LHD Experimental Group
Contributions to 28th European Physical Society Conference on Controlled Fusion and Plasma Physics (Madeira Tecnopolo, Funchal, Portugal, 18-22 June 2001) from LHD Experiment
July 2001

NIFS-710 V Yu. Sergeev, R K. Janev, M.J Rakovic, S. Zou, N. Tamura, K.V Khlopenkov and S. Sudo
Optimization of the Visible CXRS Measurements of TESPEL Diagnostics in LHD
Aug 2001

NIFS-711 M. Bacal, M Nishiura, M. Sasao, M. Wada, M Hamabe and H Yamaoka
Effect of Argon Additive in Negative Hydrogen Ion Sources
Aug. 2001

NIFS-712 K Saito, R. Kumazawa, T. Mutoh, T Seki, T Watari, T. Yamamoto, Y. Torii, N Takeuchi C Zhang, Y Zhao, A Fukuyama, F Shimpo, G. Nomura, M. Yokota, A. Kato, M. Sasao, M. Isobe, A.V. Krasilnikov, T. Ozaki, M Osakabe, K. Narihara, Y Nagayama, S. Inagaki, K. Itoh, T. Ido, S Morita, K. Ohkubo, M. Sato, S Kubo, T Shimozuma, H. Idei, Y. Yoshimura, T. Notake, O. Kaneko, Y Takeiri, Y. Oka, K. Tsumori, K. Ikeda, A. Komori, H. Yamada, H Funaba, K.Y Watanabe, S. Sakakibara, R. Sakamoto, J Miyazawa, K. Tanaka, B J Peterson, N Ashikawa, S. Murakami, T Minami, M Shoji, S Ohdachi, S Yamamoto, H. Suzuki, K Kawahata, M. Emoto, H Nakanishi, N. Inoue, N Ohyabu, Y Nakamura, S Masuzaki, S Muto, K. Sato, T. Morisaki, M Yokoyama, T. Watanabe, M. Goto, I Yamada, K. Ida, T. Tokuzawa, N Noda, K. Toi, S Yamaguchi, K. Akaishi, A Sagara, K Nishimura, K. Yamazaki, S. Sudo, Y. Hamada, O. Motojima, M. Fujiwara

A Study of High-Energy Ions Produced by ICRF Heating in LHD
Sep. 2001

NIFS-713 Y Matsumoto, S -I. Oikawa and T. Watanabe
Field Line and Particle Orbit Analysis in the Periphery of the Large Helical Device
Sep 2001

NIFS-714 S Toda, M. Kawasaki, N Kasuya, K Itoh, Y Takase, A. Furuya, M. Yagi and S -I. Itoh
Contributions to the 8th IAEA Technical Committee Meeting on H-Mode Physics and Transport Barriers (5-7 September 2001, Toki, Japan)
Oct. 2001

NIFS-715 A. Maluckov, N. Nakajima, M Okamoto, S Murakami and R Kanno
Statistical Properties of the Particle Radial Diffusion in a Radially Bounded Irregular Magnetic Field
Oct. 2001

NIFS-716 Boris V Kuteev
Kinetic Depletion Model for Pellet Ablation
Nov 2001

NIFS-717 Boris V. Kuteev and Lev D. Tsendin
Analytical Model of Neutral Gas Shielding for Hydrogen Pellet Ablation
Nov. 2001

NIFS-718 Boris V Kuteev
Interaction of Cover and Target with Xenon Gas in the IFE-Reaction Chamber
Nov 2001

NIFS-719 A. Yoshizawa, N Yokoi, S -I Itoh and K Itoh
Mean-Field Theory and Self-Consistent Dynamo Modeling
Dec. 2001

NIFS-720 V.N. Tsytovich and K Watanabe
Universal Instability of Dust Ion-Sound Waves and Dust-Acoustic Waves
Jan. 2002

NIFS-721 V.N. Tsytovich
Collective Plasma Corrections to Thermonuclear Reactions Rates in Dense Plasmas
Jan 2002

NIFS-722 S. Toda and K. Itoh
Phase Diagram of Structure of Radial Electric Field in Helical Plasmas
Jan. 2002

NIFS-723 V.D Pustovitov
Ideal and Conventional Feedback Systems for RWM Suppression
Jan 2002